



# Assessment of the photoprotective potential and structural characterization of secondary metabolites of Antarctic fungus *Arthrinium* sp.

Ana Carolina Jordão<sup>1</sup> · Gustavo Souza dos Santos<sup>1,5</sup> · Thaiz Rodrigues Teixeira<sup>1,6</sup> · Ana Júlia Pasuch Gluzezak<sup>2</sup> · Clarissa Bechuate de Souza Azevedo<sup>2</sup> · Karina de Castro Pereira<sup>2</sup> · Ludmilla Tonani<sup>3</sup> · Lorena Rigo Gaspar<sup>2</sup> · Márcia Regina von Zeska Kress<sup>3</sup> · Pio Colepicolo<sup>4</sup> · Hosana Maria Deboni<sup>1</sup>

Received: 13 September 2023 / Revised: 16 November 2023 / Accepted: 17 November 2023 / Published online: 23 December 2023  
© The Author(s), under exclusive licence to Springer-Verlag GmbH Germany, part of Springer Nature 2023

## Abstract

Interest in Antarctic fungi has grown due to their resilience in harsh environments, suggesting the presence of valuable compounds from its organisms, such as those presenting photoprotective potential, since this environment suffers the most dangerous UV exposure in the world. Therefore, this research aimed to assess the photoprotective potential of compounds from sustainable marine sources, specifically seaweed-derived fungi from Antarctic continent. These studies led to discovery of photoprotective and antioxidant properties of metabolites from *Arthrinium* sp., an endophytic fungus from Antarctic brown algae *Phaeurus antarcticus*. From crude extract, fractions A-I were obtained and compounds 1–6 isolated from E and F fractions, namely 3-Hydroxybenzyl alcohol (1), (-)-orthosporin (2), norlichexanthone (3), anomalin B (4), anomalin A (5), and agonodepside B (6). Compounds 1, 2, and 6 were not previously reported in *Arthrinium*. Fraction F demonstrated excellent absorbance in both UVA and UVB regions, while compound 6 exhibited lower UVB absorbance, possibly due to synergistic effects. Fraction F and compound 6 displayed photostability and were non-phototoxic to HaCaT cells. They also exhibited antioxidant activity by reducing intracellular ROS production induced by UVA in keratinocyte monolayers and reconstructed human skin models (resulting in 34.6% and 30.2% fluorescence reduction) and did not show irritation potential in HET-CAM assay. Thus, both are promising candidates for use in sunscreens. It is noted that Fraction F does not require further purification, making it advantageous, although clinical studies are necessary to confirm its potential applicability for sunscreen formulations.

**Keywords** *Arthrinium* · Marine Antarctic natural products · Photoprotection · Antioxidant · Reconstructed human skin

## Introduction

The marine environment is distinguished by its substantial variability in abiotic and biotic factors, encompassing high pressures, salinity, tides, depth, and temperature fluctuations. As a result, wide biological diversity and unique chemical structures have emerged, making the marine environment an important source of secondary metabolites with biotechnological applications. In the marine environment, sessile living organisms, such as sponges, cnidarians, and algae, biosynthesize these compounds to intermediate ecological

interactions, such as chemical defense mechanisms against herbivores and protection against abiotic factors, particularly high levels of ultraviolet (UV) light (Li et al. 2020).

The high exposure to UV radiation is harmful for all the organisms exposed. It is well-known that chronic exposure to UV radiation from sunlight has negative health effects, and a growing concern about such effects has caused an increase in the use of formulations containing UV filters (Watkins and Sallach 2021). Besides sunscreens, UV filters are used in more than 2,000 personal cosmetic products (Dinardo and Downs 2018; Zhang et al. 2021). The global production of UV filters is estimated to be more than 10,000 tons per year. Inevitably, these products end up being released into the aquatic environment, either directly, such as by swimming in this environment; or indirectly, such as by washing the

---

Communicated by Yusuf Akhter.

Extended author information available on the last page of the article

product off while bathing. This release is increasing concerns about the impact of the presence of these substances in the aquatic environment (Zhang et al. 2021). In vivo and in vitro studies show vast adverse effects caused to the environment and exposed organisms, such as coral reef bleaching and toxicity to the endocrine, neurological, and other systems of resident organisms (Fivenson et al. 2020). In response to these studies concerning environmental injury, some regions have banned the use of some UV filters, such as oxybenzone (benzophenone-3) and octinoxate (ethylhexyl methoxycinnamate). These bans take place in Hawaii, the US Virgin Islands, Key West in Florida, Palau, and Bonaire (Mitchellmore et al. 2021). There is a need, therefore, for eco-friendly, sustainable, and safer UV filters as alternatives to the synthetic compounds available in the cosmetic market (Fivenson et al. 2020). Several organisms, especially those exposed to intense UV radiation such as Antarctic derived organisms, have developed various photo adaptive mechanisms including production of antioxidants and UV absorbing metabolites (Saewan and Jimtaisong 2015).

The Antarctic continent is one of the most pristine and harsh ecosystems on the planet. This is due to low temperatures, low levels of organic nutrients, low water availability, strong winds, and high incidence of UV rays. However, even under these conditions, benthic algal communities and microorganisms thrive in Antarctica due to their adaptation strategies which includes the production of distinctive secondary metabolites. Numerous species of fungi have been described in association with seaweeds in parasitic, saprophytic, or endophytic relationships. These organisms are collectively known as algicolous fungi, which are specialized to grow on or in close association with algae. This fungi niche is relatively unexplored but holds great metabolic potential. Interest in Antarctic fungi, in particular, has been growing due to their ability to survive in the harsh Antarctic environment, which suggests the presence of unusual and promising biosynthetic pathways that could lead to novel bioactive compounds (Ogaki et al. 2019). These compounds are targeted for numerous biotechnological applications such as new drug leads and cosmetic ingredients (Dos Santos et al. 2021).

New cosmetic products, especially sunscreen formulations, have been developed based on marine derived secondary metabolites such as mycosporine-like amino acids (MAAs). MAAs are a class of small, water-soluble molecules that are widely distributed in various organisms, including bacteria, fungi, algae, and marine invertebrates (Vega et al. 2021). These compounds are particularly targeted due to their ability to absorb the UV rays ranging from 310 to 360 nm (Rosic 2021; Ding et al. 2022). Other carotenoids such as fucoxanthin extracted from marine seaweed might be useful for human skin photoprotection (Tavares et al. 2020a, b). Furthermore, some other natural

compounds were reported as having anti-UV activity, such as phenolic compounds. In nature, phenolic compounds are biosynthesized to balance ROS production and present protective effects against DNA damage induced by UV radiation (Bedoux et al. 2014; Ding et al. 2022). Antarctica experiences high UV radiation, especially during the southern summer, and the persistence of the Antarctic ozone hole, despite efforts to reduce ozone-depleting substances, continues to be a concern. The severity of ozone depletion is strongly influenced by weather conditions and is particularly pronounced in late spring (Cordero et al. 2022). Consequently, Antarctic organisms have been compelled to produce photoprotective compounds (Núñez-Pons et al. 2018).

The genera *Arthrimum* is part of the Apiosporaceae family in the Ascomycota phylum. Currently, there are 88 species recognized worldwide. *Arthrimum* strains have mostly been recovered from regions characterized by temperate or cold climates such as the Antarctic Peninsula (Overgaard et al. 2023; Pintos and Alvarado 2021). Species within these genera exhibit diverse ecological roles, from saprotrophy, pathogenicity, to endophytic associations and have been isolated from assorted hosts, including plants and seaweeds (Heo et al. 2018). Overall, in response to the growing demand for safer and environmentally friendly sunscreen ingredients, this study aims to assess interesting metabolites produced by the Antarctic fungus *Arthrimum* sp. Our goal is to identify a novel UV-filtering compound with low toxicity and minimal ecological impact, employing analytical, spectrometric and spectroscopic and biological assays to evaluate its potential as a sunscreen ingredient.

*Arthrimum* species are known to produce a varied classes of compounds such as alkaloids, peptides, terpenes, coumarins, xanthenes and pyrones. These secondary metabolites exhibit a wide range of promising biological activities, including antibacterial, antifungal, anti-inflammatory, anti-cancer, and antioxidant properties. However, the photoprotective potential of compounds produced by *Arthrimum* species is scarce. Overall, in response to the growing demand for safer and environmentally friendly sunscreen ingredients, this study aims to assess the metabolites generated by the Antarctic fungus *Arthrimum* sp. Our goal is to identify a novel UV-filtering compound with low toxicity and minimal ecological impact, employing analytical techniques and biological assays to evaluate its potential as a sunscreen ingredient.

## Materials and methods

### Fungal isolation

Initially, a health specimen of the seaweed *Phaeurus antarcticus* was collected at Greenwich Island, Antarctica

(62°26'46.9" S 59°44'20.3" W) in November/2015 during the Brazilian Antarctic Expedition OPERANTAR XXXIII. The seaweed was rinsed in sterile seawater to remove adherent debris and other contaminants. To the selective isolation of fungal endophytes, the seaweed was cut into small fragments (0.5–1.5 cm) and surface disinfected by immersion in 70% ethanol (v/v) for 15 s, followed by rinsing in sterile seawater three times. Control plates were used to assess the efficiency of the disinfection procedure. The disinfected fragments were used to make imprints on the agar surface (Control 1) and then inoculated in another Petri dish containing an isolation medium for up to 60 days. Control 2 consisted of the inoculation of water drops from the third rinsing procedure (Teixeira et al. 2019). The seaweed was inoculated, aiming the endophytic fungi to grow, in a medium consisted of potato dextrose agar (39 g/L) prepared in sterile seawater supplemented with 200 mg/L of chloramphenicol (Sarasan et al. 2017). The emerging colony was purified by streaking technique and preserved in flasks containing glycerol or mineral oil, in the Laboratory of Marine Environment Organic Chemistry and at  $-80^{\circ}\text{C}$  in Laboratory of Clinical Mycology, both in School of Pharmaceutical Sciences of Ribeirão Preto, University of São Paulo, Brazil.

### Fungal identification

To the DNA extraction procedures, the isolated fungal strain was cultivated in potato dextrose broth. The identification was carried based on the sequencing of the internal transcribed sequence (ITS) region of the fungal ribosomal DNA. The polymerase chain reactions (PCR) were performed with Phusion<sup>®</sup> High-Fidelity DNA Polymerase (New England BioLabs, Inc.) and primers ITS1 (5'-T C C GTA GGT GAA CCT GCG G-3') and ITS4 (5'-TCC TCC GCT TAT TGA TAT GC-3') (White et al. 1990). The PCR products were purified with Wizard<sup>®</sup> SV Gel and PCR Clean-Up System (Promega) and sequenced using the same primers with ABI3730 DNA Analyzer (Applied Biosystems). Each sequence was analyzed with ChromasPro<sup>®</sup> Software (ChromasPro 1.7.6, Technelysium Pty Ltd., Tewantin QLD, Australia). The sequences were then tested against the publicly available DNA sequences in the National Institutes of Health (NIH) genetic sequence database (Benson et al. 2013).

### Fermentation and extraction

The fungus was grown in Potato Dextrose Agar medium (PDA NEOGEN<sup>®</sup>, USA, 39 g/L) for 7 days. After this period, 10 plugs (5 mm diameter) were transferred to each of the 50 Erlenmeyer flasks (500 mL), containing 200 mL of Potato Dextrose Broth (PDB KASVI<sup>®</sup>, BRAZIL, 27 g/L) medium, prepared in artificial seawater SWBG-11 described by Castenholz 1988. The flasks remained

static and at room temperature for 14 days. Liquid–liquid extraction with ethyl acetate was performed to obtain the extracts, adding 100 mL of the solvent in each Erlenmeyer flask followed by 5 min in the ultrasonic bath (75 W). The procedure was performed 3 times for each flask. After the method was completed, the aqueous culture medium was properly discarded. The crude extract (CE) was concentrated in a rotary evaporator under reduced pressure and heat, not exceeding the temperature of  $28^{\circ}\text{C}$ .

### Crude extract fractionation and compounds isolation

The CE (1.2 g) was fractionated by vacuum liquid chromatography (VLC) method, using a stationary phase silica gel (40–70 mesh, Merck) in a 200 mL glass Buchner funnel (18 mm diameter, 250 mm height). Elution using the organic solvents *n*-hexane (Hex), ethyl acetate (EtOAc) and methanol (MeOH) with 200 mL of a stepwise polarity gradient yielded nine fractions: VLC A (Hex 100%), VLC B (Hex:EtOAc 9:1), VLC C (Hex:EtOAc 4:1), VLC D (Hex:EtOAc 3:2), VLC E (Hex:EtOAc 2:3), VLC F (Hex:EtOAc 1:4), VLC G (EtOAc 100%), VLC H (EtOAc:MeOH 7.5:2.5) and VLC I (MeOH 100%).

Fraction E and F were submitted to purification by reverse phase HPLC (LC-6AD model, Shimadzu) coupled with diode array detector (SPD-M10A model, Shimadzu) with a semi-preparative column C-8 (25 cm  $\times$  10 mm, 10  $\mu\text{m}$ —Ascentis Supelco, USA). In this isolation, a polarity gradient method changing concentration of MeOH in distilled water: 15% (0 min)—100% (20–22 min)—15% (23–25 min) was used.

### Structure identification

The isolated compounds were characterized through spectrometry analyses, such as mass spectrometry (MS) and nuclear magnetic resonance (NMR). The MS data were obtained using a spectrometer of Bruker, microTOF Q II with electrospray ionization and analyzer time of flight type (TOF) in Organic Chemistry Laboratory (FCFRP-USP). The NMR spectroscopy was employed to get data from unidimensional ( $^1\text{H}$ ) and bi-dimensional (HMBC, HSQC) analyses. The NMR spectra were acquired in Chemistry Department of Faculty of Philosophy, Sciences and Letters at Ribeirão Preto—USP, using a spectrometer model DRX 500, Bruker, Billerica operating at 500 MHz, using deuterated solvents from Sigma-Aldrich: methanol ( $\text{CD}_3\text{OD}$ ), dimethyl sulfoxide ( $\text{DMSO}-d_6$ ) and chloroform ( $\text{CDCl}_3$ ). The obtained results were compared with literature data.

## Determination of the UV absorption spectra

Absorption spectra in the UV region of the CE, fractions and isolated compounds were determined by a spectrophotometer (Agilent 8453) in the 200–400 nm range, for the determination of the UV absorption spectra. The samples were diluted in methanol to yield a solution with a concentration of 100 µg/mL. However, the samples that showed higher absorbance in the UVA-UVB region were analyzed in the further studies (photostability, phototoxicity and antioxidant).

## Photostability test

For the photostability studies, 1 mL of each solution sample was added to glass beakers and then subjected to solvent evaporation until a dried film was obtained. The samples were then submitted or not to UV radiation of 4 mW/cm<sup>2</sup> emitted from a Philips UVA lamp Actinic BL/10 (Eindhoven, the Netherlands) (cumulative dose of 27.5 J/cm<sup>2</sup>) measured with a Dr. Hönle radiometer (Planegg, Germany) equipped with a UVA sensor. After irradiation, the dried film was re-suspended in 1 mL of solvent, and the absorption spectrum of the solutions in the 280–400 nm range was analyzed. The area under the curve (AUC), which is the integral of the absorption spectrum of the samples in the UVB (280–320 nm) and UVA (320–400 nm) ranges, were used to calculate the photostability using the integration function of the MicroCal OriginPro Software (8 SRO, OriginLab Corporation, Northampton, MA, USA). The results of the photostability experiments are expressed as a percentage of the area of irradiated samples related to the area of non-irradiated samples, considered as 100% (Gaspar and Maia Campos 2006; Tavares et al. 2020a, b).

In addition, the UVA/UVB ratio and the Boots star rating, which indicate broad-spectrum protection, were studied. The Boots star rating system is based on measurement of UV transmittance through a sunscreen film. The initial absorbance curve is obtained; then each sample is irradiated and the final absorbance curve is obtained. The mean absorbance values (AUC) in the UVA range from 320 to 400 nm and the UVB range from 290 to 320 nm are determined before and after irradiation. The ratios of mean UVA to UVB absorbance measured before and after irradiation were used to determine the Boots star rating (no star: < 0.6, 3: > 0.6, 4: > 0.8, 5: > 0.9) (Wang et al. 2008).

## Toxicity assessment

### Phototoxicity assay (3T3 NRU-PT)

The selected fraction (F) and compound **6** (agonodepside B) were submitted to a phototoxicity test based on neutral

red (Merck, Darmstadt, Germany) uptake using 3T3 fibroblasts according to Organization for Economic Co-operation and Development (OECD) n° 432 guideline (OECD, 2019). The fibroblasts were cultivated in Dulbecco's modified Eagle medium (DMEM, Carlsbad, CA, USA) supplemented with newborn calf serum (10%, Carlsbad, CA, USA), glutamine (4 mM), penicillin (100 IU/mL) and streptomycin (100 µg/mL) from Sigma Aldrich (St. Louis, MO, USA). In this test 3T3 Balb/c fibroblasts seeded on two 96-well plates (1 × 10<sup>4</sup> cells/well) were pre-incubated with eight different concentrations ranging from 6.81 to 100 µg/mL of the samples analyzed for 1 h. Norfloxacin (St. Louis, MO, USA) was used as positive control. One plate was then exposed to a UVA irradiation dose of 9 J/cm<sup>2</sup>, using irradiance of 6.8 mW/cm<sup>2</sup> for 22 min obtained with a solar simulator (Dr. Hönle type SOL-500, Planegg, Germany), while another one was kept in the dark. To evaluate the cyto- and phototoxicity of the samples, cell viability in the presence and absence of radiation was determined by the neutral red uptake method. Data were analyzed using Phototox Software 2.0, which calculated the Mean Photo Effect (MPE). According to the phototoxicity determination guideline recommended by OECD (OECD, 2019), sample with MPE < 0.10 predicts “no phototoxicity”, while MPE > 0.10 and < 0.15 predict “equivocal phototoxicity”; and MPE > 0.15 predicts “phototoxicity”.

### Ocular irritation potential (HET-CAM assay)

The Hen's egg test-chorioallantoic membrane (HET-CAM) assay was performed according to Luepke and Kemper (1986). Fertilized White Leghorn chicken eggs at the tenth day of incubation at 37 °C under 50–60% relative humidity were used. The eggshell around the air space was removed, the inner membrane was hydrated with a 0.9% NaCl solution and removed carefully, and the chorioallantoic membrane (CAM) was exposed. Three hundred µL of a 0.01% solution (100 µg/mL) of samples (fraction F and compound **6**) were applied to the CAM and 20 s after, the CAM was rinsed off with 5 mL of 0.9% NaCl solution and monitored for 5 min using a stereo microscope (SZT-Led#, Bel Photonics, Brazil), in order to observe the irritant events such as hyperemia, hemorrhage and coagulation. It was given one score for each observed effect, according to the time of appearance, where a sample is classified as non-irritant if presents the following Irritation Score (IS): 0 ≤ IS ≤ 0.9 for slightly irritant if 1.0 ≤ IS ≤ 4.9; for moderate irritant if 5.0 ≤ IS ≤ 8.9 and as severe irritant if 9.0 ≤ IS ≤ 21, respectively, (Table 1). The IS was obtained by the sum of individual scores of hyperemia, hemorrhage and coagulation. A 1% (w/w) sodium lauryl sulfate (SDS) solution was used as positive control and a 0.9% sodium chloride (NaCl) solution was used as negative control. The test was performed in quadruplicate.

**Table 1** Scores given to the irritant events observed in the HET-CAM test (adapted from Luepke and Kemper, 1986)

Irritant Event	0–30 s	30 s–2 min	2 min–5 min
Hyperemia	5	3	1
Hemorrhage	7	5	3
Coagulation	9	7	5

### Photoprotection against UVA-induced ROS production

**HaCat antioxidant activity** The quantification of intracellular ROS produced by HaCaT cell exposure to UVA was evaluated using the 2',7'-dichlorodihydrofluorescein diacetate (DCFH<sub>2</sub>-DA, Sigma Aldrich, St. Louis, MO, USA) probe, a non-fluorescent compound that permeates the cell, is hydrolyzed by intracellular esterases and, oxidized by ROS to the fluorescent compound, 2'-7'-DCF (Kalyanaraman et al., 2011). UVA irradiation provokes ROS generation, which can oxidize DCFH to dichlorofluorescein, a fluorescent product, increasing fluorescence (%).

Prior to the beginning of the assay, cell viability was evaluated to exclude the possibility that the decrease in fluorescence intensity obtained in the ROS assay is related to cell death and not to antioxidant activity. The assay was performed under the same conditions (cell type, density, and exposure times) as the measurement of intracellular ROS generation in HaCaT monolayers cells.

Cell viability was evaluated using keratinocytes HaCaT (Cell Bank of Rio de Janeiro, Rio de Janeiro, Brazil), which were cultivated in DMEM (Gibco, Carlsbad, CA, USA) supplemented with fetal bovine serum (10%, Gibco, Carlsbad, CA, USA), pyruvate (1 mM), penicillin (100 IU/mL) and streptomycin (100 µg/mL) from Sigma Aldrich (St. Louis, MO, USA). Subsequently, they were seeded in 96-well plates ( $1 \times 10^5$  cells/well) and cultured overnight at 37 °C in a 5% CO<sub>2</sub> atmosphere. The cells were treated with the samples selected for this experiment, fraction F and isolated compound **6**, as it showed the best UV absorbance among the isolated compounds, using concentrations of 10.0; 5.0 and 2.5 µg/mL. The cells were incubated for 1 h. Then, cell viability was determined by neutral red uptake (Rangel et al. 2020; Gaspar, Maia Campos and Liebsch, 2013). Sodium dodecyl sulfate (SDS) was used as a positive cytotoxic control (100 µg/mL). The absorbance of untreated cells was considered as 100% to calculate the percentage of cell viability relative to the samples.

For the evaluation of photoprotection against UVA-induced ROS production, HaCaT cells cultivated in supplemented DMEM were seeded in 96-well plates ( $1 \times 10^5$  cells/well) and cultured overnight at 37 °C in a 5% CO<sub>2</sub> atmosphere. The cells were treated and incubated with sample (compound **6** at 10.0; 5.0 and 2.5 µg/mL) for 1 h, then

they were incubated with DCFH<sub>2</sub>-DA (10 µM) for 30 min, followed by exposure to UVA radiation (Solar simulator Dr. Hönle type SOL-500, Planegg, Germany) with a total dose of 4 J cm<sup>-2</sup>, using an irradiance of 6.6 mW/cm<sup>2</sup> for 10 min. Quercetin (10 µg/mL) and norfloxacin (100 µg/mL) (Sigma Aldrich, St. Louis, MO, USA) were used as ROS quencher and generator, respectively. The fluorescence was determined with a microplate reader (Synergy™ HT, BioTek, USA) at 485 nm excitation and 528 nm emission. The fluorescence of untreated irradiated cells was considered to be 100% in order to calculate the relative percentage of samples.

**Reconstructed Human Skin Model (RHS) antioxidant activity** The assay with *in house* reconstructed skin models was conducted after approval by the Ethics Committee in Research Involving Human Beings—School of Pharmaceutical Sciences of Ribeirão Preto—USP (CAAE number 31758619.5.0000.5403), using primary human fibroblasts and keratinocytes from foreskin (pooled from three donors). Informed written consent was obtained from all the donors or their parents or legal guardians.

Primarily, the dermal compartment was prepared by seeding  $1.14 \times 10^5$  normal human fibroblasts with collagen type I (Corning®) into the insert (0.4 µm pore size; ThinCert™, Greiner Bio-One GmbH, Frickenhausen—Germany) and incubated for 20 h. After that,  $3.7 \times 10^5$  normal human keratinocytes were seeded on the top of the dermal compartment and kept submerged in an *in house* prepared culture medium for 24 h, so the cells could form a monolayer. Throughout 7 days, the culture was maintained at the air–liquid interface allowing complete keratinocytes differentiation and stratification, and the culture medium was changed every other day (Pennacchi et al 2015; Pivetta et al 2019; Tavares et al 2020a, b)..

After the skin models were fully differentiated on day 10, the measurement of intracellular ROS generation began with the incubation of the models with the DCFH<sub>2</sub>-DA (50 µM) for 45 min in the absence of light. After washing with phosphate-buffered saline (PBS), 25 µL of the sample were applied onto the skin models for 1 h and then, subjected (UV+) or not (UV−) to 10 J.cm<sup>-2</sup> of UVA radiation from a SOL-500 solar simulator (Dr Honle AG, Planegg, Alemanha).

Immediately after irradiation and washing with PBS, the tissues were frozen in liquid nitrogen and the, 8 µm histological sections were obtained in a cryostat. Pictures were obtained in an inverted Ti-S microscope (Nikon Instruments Inc., Holland), 488 nm, using 100 ms of exposure intensity and analyzed by Image J software (Marionnet et al. 2014; Rasmussen et al. 2010). Fluorescence intensity results were normalized to area/pixels and expressed as percent fluorescence compared to untreated irradiated (UV+) control.

## Statistical analysis

The results were analyzed by one-way ANOVA followed by Tukey's post hoc test using Minitab version 18.1, since they presented normal distribution (Anderson–Darling test). *p*-Values lower than 0.05 were considered to be statistically significant.

## Results and discussion

### Fungal identification

The fungal isolate was obtained from the fragments of *Phaeurus antarcticus* and was later identified as the fungus *Arthrinium* sp. The results of the identification process can be observed in Table 2, as well as the NCBI reference and accession number.

### Compound's identification and characterization

Fraction E, obtained from CE of *Arthrinium* sp. was selected to perform metabolite isolation due to its non-complex chromatogram and sample amount, which makes it easier to isolate metabolites. Additionally, fraction F, although did not show a simple chromatogram profile, it was also selected once in a bio-guided assay showed best UV absorbance

among the other fractions, discussed later in this article. So, it was possible to submit the fraction E (contained 180.0 mg) and F (contained 141.0 mg) to HPLC separation to yield the compounds **1**, **3**, and **6**, and the compounds **2**, **4**, **5**, and **6**, respectively (Fig. 1, 1–6). The report of compounds **1**, **2** and **6** is unprecedented in species of *Arthrinium*.

Compound **1** (2.0 mg) was obtained as a colorless liquid with  $\lambda_{\max}$  273 and 324 nm. Its molecular formula was established as  $C_7H_8O_2$  based on high resolution mass spectrometry (HRMS, ESI),  $m/z$  123,0484 [M-H]<sup>-</sup>. The full structure was determined by <sup>1</sup>H NMR analyses (500 MHz, CDCl<sub>3</sub>, ppm) by observing chemical shifts ( $\delta$ ): 4.66 (2H, *s*, H-7), 6.76 (1H, *dd*,  $J=7.7, 2.3$  Hz, H-6) 6.87 (1H, *br s*, H-2), 6.92 (1H, *d*,  $J=7.7$  Hz, H-4), 7.23 (1H, *t*,  $J=7.7$  Hz H-5) and <sup>13</sup>C NMR (HMBC, HSQC; 500 MHz, CD<sub>3</sub>OD, ppm)  $\delta$ : 142.7 (C, C-1), 113.4 (CH, C-2), 157.1 (C, C-3), 114.0 (CH, C-4), 128.8 (CH, C-5), 117.4 (C, C-6), 63.5 (CH<sub>2</sub>, C-7). The identity of the compound was confirmed after data comparison with the literature of Alfaro et al. 2003, proving to be 3-Hydroxybenzyl alcohol (Fig. 1, 1).

Compound **2** (1.0 mg) was obtained as a white powder with  $[\alpha]_D^{26} - 0.63^\circ$  and  $\lambda_{\max}$  244, 238, 277 and 326 nm. Its molecular formula was established as  $C_{12}H_{12}O_5$  based on HRMS (ESI),  $m/z$  235,0756 [M-H]<sup>-</sup>. The full structure was determined by <sup>1</sup>H NMR analyses (500 MHz, DMSO-*d*<sub>6</sub>, ppm)  $\delta$ : 1.12 (3H, *d*,  $J=6.2$  Hz, H-11), 2.59 (2H, *m*, H-9), 3.96 (1H, *m*, H-10), 4.80 (1H, *d*,  $J=4.9$  Hz, OH-10), 6.29

**Table 2** Results concerning the fungal identification, NCBI reference and accession

Code	Score	E-value	Identities	Final identification	Reference NCBI Accession	NCBI Accession
LMC8101	937	0.0	98%	<i>Arthrinium</i> sp.	JQ411349.1	OR412386

**Fig. 1** Major compounds isolated from antarctic *Arthrinium* sp. extract

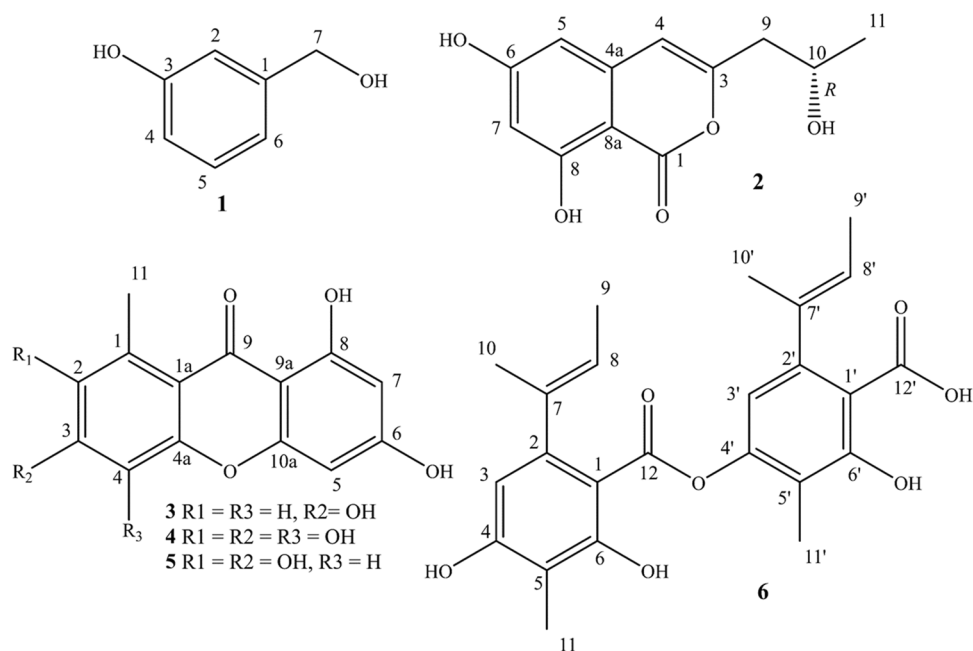
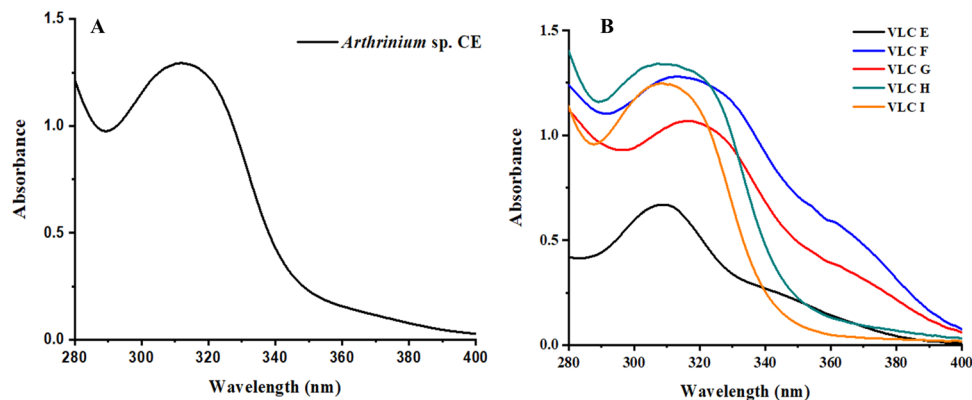


**Fig. 2** Absorption spectra of the crude extract (CE) (A) from *Arthrinium* sp. fungus and the obtained fractions (B)



(1H, *d*, *J* = 2.0 Hz, H-5), 6.35 (1H, *d*, *J* = 2.0 Hz, H-7), 6.47 (1H, *s*, H-4), 10.98 (1H, *s*, OH-8). The identity of the compound was confirmed after data comparison with the literature of Gremaud et al., 1994, proving to be 6,8-Dihydroxy-3-[(2R)-2-hydroxypropyl]-1H-2-benzopyran-1-one, also known as (-)-orthosporin (Figs. 1, 2).

Compound **3** (4.0 mg) was obtained as a light yellow amorphous solid with  $\lambda_{\max}$  241 and 311 nm. Its molecular formula was established as  $C_{14}H_{10}O_5$  based on HRMS (ESI),  $m/z$  257,0459 [M-H]<sup>-</sup>. The full structure was determined by <sup>1</sup>H NMR analyses (500 MHz, CD<sub>3</sub>OD, ppm)  $\delta$ : 2.76 (3H, *s*, H-11), 6.09 (1H, *d*, *J* = 2.0, H-7), 6.21 (1H, *d*, *J* = 2.0, H-5), 6.58 (1H, *br s*, H-2), 6.59 (1H, *br s*, H-4) and <sup>13</sup>C NMR (HMBC, HSQC; 500 MHz, CD<sub>3</sub>OD, ppm)  $\delta$ : 143.2 (C, C-1), 111.3 (C, C-1a), 115.5 (CH, C-2), 157.1 (C, C-3), 100.1 (CH, C-4), 159.7 (C, C-4a), 96.9 (CH, C-5), 164.2 (C, C-6), 97.4 (CH, C-7), 162.7 (C, C-8), 102.3 (C, C-9a), 164.6 (C, C-10a), 23.1 (CH<sub>3</sub>, C-11). The identity of the compound was confirmed after data comparison with the literature of Abdel-Lateff et al. 2003, proving to be 3,6,8-trihydroxy-1-methylxanthone, also known as norlichexanthone (Figs. 1, 3).

Compound **4** (1.0 mg) was obtained as a yellow amorphous solid with  $\lambda_{\max}$  258 and 327 nm. Its molecular formula was established as  $C_{14}H_{10}O_7$  based on HRMS (ESI),  $m/z$  289,0519 [M-H]<sup>-</sup>. The full structure was determined by <sup>1</sup>H NMR analyses (500 MHz, DMSO-*d*<sub>6</sub>, ppm)  $\delta$ : 2.58 (3H, *s*, H-11), 6.07 (1H, *d*, *J* = 2.0, H-7), 6.30 (1H, *d*, *J* = 2.0, H-5), 13.61 (1H, *s*, OH-8). The identity of the compound was confirmed after data comparison with the literature of Abdel-Lateff et al. 2003, proving to be 2,3,4,6,8-pentahydroxy-1-methylxanthone, also known as anomalin B (Figs. 1, 4).

Compound **5** (2.0 mg) was obtained as a light yellow amorphous solid with  $\lambda_{\max}$  239, 254, 313 and 359 nm. Its molecular formula was established as  $C_{14}H_{10}O_6$  based on HRMS (ESI),  $m/z$  273,0550 [M-H]<sup>-</sup>. The full structure was determined by <sup>1</sup>H NMR analyses (500 MHz, DMSO-*d*<sub>6</sub>, ppm)  $\delta$ : 2.64 (3H, *s*, H-11), 6.07 (1H, *d*, *J* = 2.0, H-7), 6.22 (1H, *d*, *J* = 2.0, H-5), 6.67 (1H, *s*, H-4), 13.65 (1H, *s*,

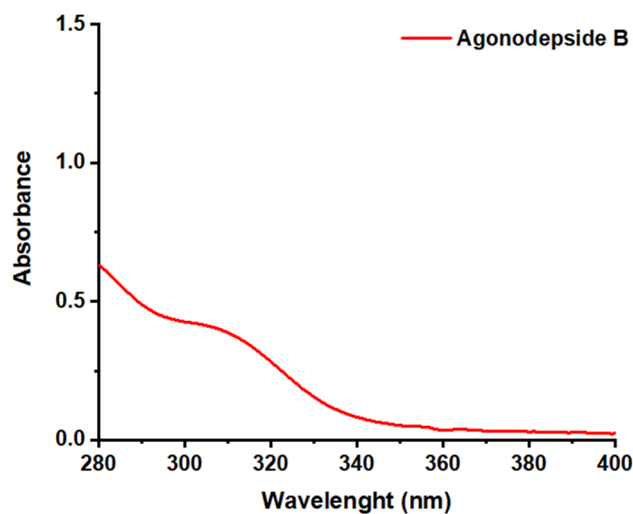


**Fig. 3** Absorption spectra of agonodepside B (**6**) in the UVB-UVA range

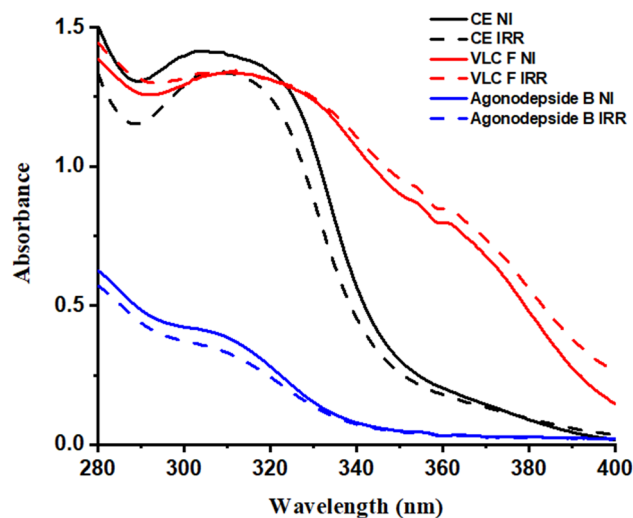


**Fig. 4** Absorption spectra of the CE, fraction F and agonodepside B (**6**), irradiated (IRR) and non-irradiated (NI)

OH-8). The identity of the compound was confirmed after data comparison with the literature of Abdel-Lateff et al. 2003, proving to be 2,3,6,8-tetrahydroxy-1-methylxanthone, also known as anomalin A (Figs. 1, 5).

Compound **6** (5.5 mg) was obtained as a strong yellow amorphous solid with  $\lambda_{\max}$  217 and 277 nm. Its molecular formula was established as  $C_{24}H_{26}O_7$  based on HRMS (ESI),  $m/z$  425.1686  $[M-H]^-$  and fragmentation (MS/MS):  $m/z$  425  $[M-H]^-$ , 221, 203. The full structure was determined by  $^1H$  NMR analyses (500 MHz,  $CDCl_3$ , ppm)  $\delta$ : 1.66 (3H, *dd*,  $J=6.8$  Hz, 1.0, H-9), 1.79 (3H, *dd*,  $J=6.8$ , 1.0 Hz, H-9'), 1.92 (3H, *br d*,  $J=1.0$  Hz, H-10'), 1.97 (3H, *br d*,  $J=1.0$  Hz, H-10), 2.04 (3H, *s*, H-11'), 2.14 (3H, *s*, H-11), 5.36 (1H, *m*, H-8), 5.65 (1H, *m*, H-8'), 6.21 (1H, *s*, H-3), 6.38 (1H, *s*, H-3'), 11.37 (1H, *s*, OH-6), 11.84 (1H, *s*, OH-6') and  $^{13}C$  NMR (HMBC, HSQC; 500 MHz,  $CDCl_3$ , ppm)  $\delta$ : 102.7 (C, C-1), 146.2 (C, C-2), 104.4 (CH, C-3), 148.6 (C, C-4), 106.8 (C, C-5), 153.2 (C, C-6), 137.2 (C, C-7), 121.4 (CH, C-8), 13.4 (CH<sub>3</sub>, C-9), 18.8 (CH<sub>3</sub>, C-10), 7.5 (CH<sub>3</sub>, C-11), 109.5 (C, C-1'), 144.3 (C, C-2'), 114.0 (CH, C-3'), 146.2 (C, C-4'), 118.3 (C, C-5'), 158.8 (C, C-6'), 137.9 (C, C-7'), 126.1 (CH, C-8'), 13.8 (CH<sub>3</sub>, C-9'), 18.5 (CH<sub>3</sub>, C-10'), 8.9 (CH<sub>3</sub>, C-11'), 162.9 (C, C-12'). The identity of the compound was confirmed after data comparison with the literature of Cao et al. 2002, proving to be agonodepside B (Figs. 1, 6).

Herein, we successfully characterized compounds from different classes commonly biosynthesized by endophytic fungi, including xanthenes, isocoumarins, and depsides. These findings highlight the metabolic diversity that *Arthrinium* has and its biotechnological and pharmaceutical potential.

Isocoumarins (compound **2**) mainly derived from the polyketide pathways, are abundant in fungi and have several biological activities, such as antifungal, anti-inflammatory, cytotoxic, and antimicrobial (Pal et al. 2011; Saeed 2016; Noor et al. 2020). Regardless of the metabolic process, most fungal isocoumarins are always characterized by a C-3 carbon substituent, as we can see in the present study for the

compound **2** ((-)-orthosporin). According to Song and co-workers (2017), this is the spontaneous outcome of a biosynthetic intramolecular cyclization, which makes the residual polyketide chain a substituent.

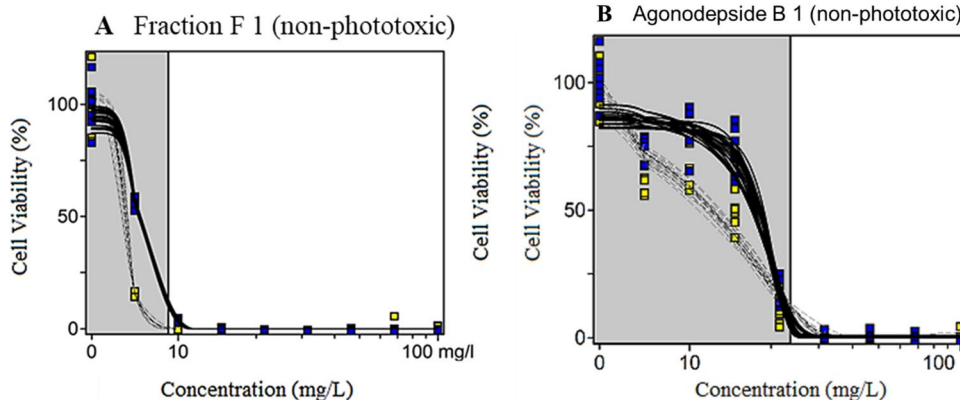
Xanthenes (compounds **3–5**) are natural polyphenolic products. The biosynthetic pathways of these compounds when produced by fungi are distinct from those produced by plants. Birch and Donovan (1953) suggested at first the biogenesis of xanthenes production by fungi. Roberts, in 1961, studied this assembly in more detail, through radiolabeled acetate feeding experiments, concluding that polyketides, from malonyl and acetyl CoA, are the precursors of the fungi's xanthenes (Badiali et al. 2023). The bioactivity of these compounds depends on the nature and/or positions of their substituents, which makes these structures unique with the possibility of binding to a variety of targets and presenting different biological activities, including antimicrobial, antioxidant, and cytotoxic (El-Seedi et al. 2010; Le Pogam and Boustie 2016).

Finally, agonodepside B (compound **6**) is a depside that was isolated for the first time from the terrestrial filamentous fungus F7524 (Cao et al. 2002). Depsides are natural products formed by phenolic units, biosynthetically originated from the condensation of orselinic acid and derivatives of orcinol or two units of orselinic acid through the formation of an ester by the polyketide synthase (PKS) itself or by a separate enzyme (Kealey et al. 2021; Legaz et al. 2011).

## Determination of the UV Absorption Spectra



The crude extract (CE) (Fig. 2A) and fractions E-I (Fig. 2B) presented a good absorption of the UVA and UVB region indicating the presence of compounds of interest for photoprotective activity. Fraction F (contained 141.0 mg) and fraction G (contained 72.0 mg) fractions presented absorbance in both UVB (280–320 nm), UVA I and II (320–400 nm) ranges. The fractions H (contained 370.0 mg) and I (contained 155.0 mg) also presented a good absorption in the UVA II and UVB regions, which were lower than fraction

**Fig. 5** The dose–response curves of fraction F (**A**) and agonodepside B (**6**) (**B**) obtained by the 3T3 NRU phototoxicity test and plotted using the Phototox 2.0 software program. The blue and yellow dots refer, respectively, to non-irradiated cells (–UV) and irradiated ones (+UV). Evaluated doses: 6.81, 10, 14.7, 21.4, 31.6, 46.4, 68.1 and 100  $\mu\text{g}\cdot\text{mL}^{-1}$



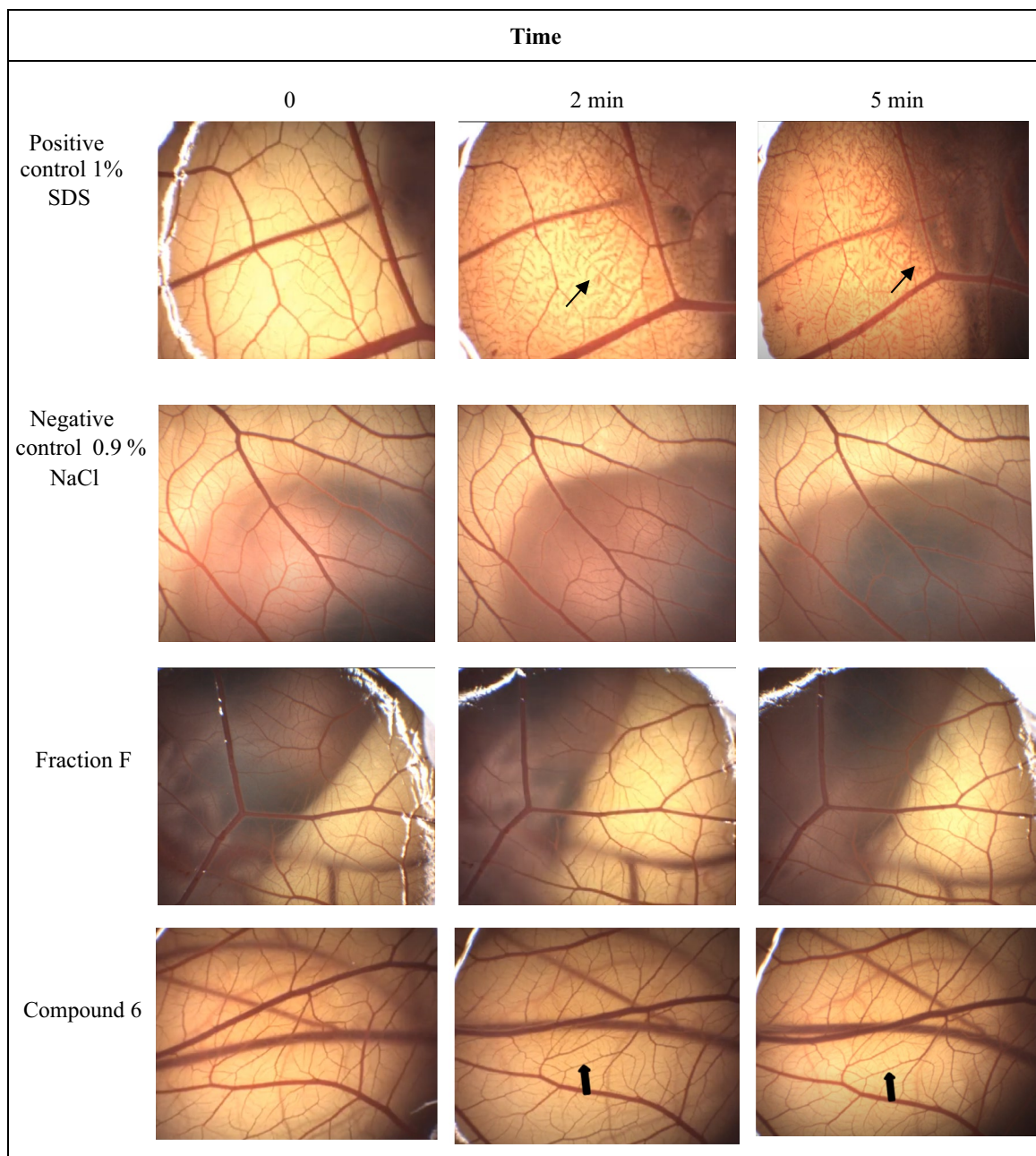




**Fig. 6** Evaluation of the irritant potential of 0.01% Fraction F and 0.01% Compound 6 by the HET-CAM assay. All images were obtained with 7× magnification. The  indicates hyperemia and  indicates hemorrhage

F (mainly in the UVA region). Fraction E exhibited lower UVB absorbance than the fractions previously mentioned. However, we chose to study it first due to its simpler metabolite isolation methodology when compared to fractions G, H, and I; and also by purpose of sample amount.

The isolated compound agonodepside B (Fig. 3) showed an average UV absorbance even more pronounced when compared to the studied extract (Fig. 2a) and fractions VLC F, G, H and I (Fig. 2b). This result may be due to synergism, which occurs when substances in mixtures show a better

biological activity than when isolated. To proceed with our investigation of the isolated compounds, we selected agonodepside B (6) due to its majority in both fractions E and F, resulting in the highest mass (5.5 mg) following purification through HPLC. While we did not attain the requisite mass for the remaining compounds necessary to conduct our photoprotection experiments, the choice of agonodepside B (6) was essential. These additional experiments are of great importance and are indispensable. We searched for a complete compound that would not only absorb UV rays

but also possess antioxidant properties. Ensuring its safety for skin use and viability for inclusion in cosmetic formulations is critical as well. The compound's UV spectra can be observed in Fig. 3.

Although agonodepside B (**6**) absorbance was not as promising as fraction F, the use of this substance as an UV filter should not be discarded. The compound may not exert a potent activity when used alone, but it can be studied to be used in combination with other natural products, or with UV filters already on the market, in order to enhance this effect, as shown in the study by Tavares et al. (2020a, b). In this work, the addition of fucoxanthin in a sunscreen formulation increased its photoprotective potential by 72%. Other studies also show the potential of natural products in association with commercial UV filters, enhancing the SPF and maintaining the safety of sunscreens. As another example, Fernandes and collaborators (2015) studied the association of benzophenone-3 with extracts of an antarctic moss (*Sanionia uncinata*), and found that its aqueous extract significantly increased the SPF of the active compound. In addition, they observed an absence of cytotoxicity (Fernandes et al. 2015; He et al. 2021).

### Photostability studies

The crude extract and the fraction with the highest absorbance in the UVB and UVA I and II regions, as well as agonodepside B (**6**), were submitted to the photostability study. All samples tested in this study were considered photostable, because their UVA and UVB absorption did not present a high reduction after irradiation. These results are shown in Fig. 4 and Tables 3 and 4. The results presented in Table 4 shows that avobenzone and fraction F presented the same boot star rating; however, AVO presented a reduction from 5 to 4, indicating photo instability. These results are in line with the literature that indicates avobenzone as a broad-spectrum and photo-unstable UV filter (Rangel et al. 2020; Scarpin et al. 2021). The UVB and UVA II filter benzophenone-3 presented a lower Boot's star rating than Fraction F.

**Table 3** Remaining percentage of the area under the curve of the irradiated samples compared to non-irradiated samples considered as 100% in the UVA and UVB range of the CE, fraction F, and agonodepside B (**6**)

Sample	Remaining percentage of the area under the curve		Stability
	UVA	UVB	
CE	87.92%	92.52%	Photostable
Fraction F	103.58%	100.88%	Photostable
Agonodepside B ( <b>6</b> )	105.35%	94.27%	Photostable

**Table 4** Boot's star rating system: ratio of UVA absorbance to UVB absorbance of the CE, fraction F, and agonodepside B (**6**) (no star: <0.6, 3:>0.6, 4:>0.8, 5:>0.9)

Sample	UVA/UVB ratio		Rating
	Non-irradiated	Irradiated	
CE	0.56	0.53	No star
Fraction F	1.18	1.19	5
Agonodepside B ( <b>6</b> )	0.26	0.31	No star
Avobenzone	4.3	0.88	5 (–UV) and 4 (+UV)
Benzophenone-3	0.73	0.65	3

The photostability obtained for the compounds studied in this work were remarkable when compared to the photo-unstable UV filters currently available in the market. Contrary to these higher photo-unstable compounds, the fractions and isolated compound **6** in our study demonstrated considerably less degradation when exposed to UV radiation. A comprehensive study by Rangel and co-workers (2020) focused on the photostability of some market-based UV filters. The results were notable, with benzophenone-3 suffering approximately 30% of UV absorption reduction, and the broad-spectrum UV filter avobenzone showing a considerable decrease (about 90% reduction) of UV absorption after exposure to UVA radiation (Rangel et al. 2020; Scarpin et al. 2021).

Photochemical reactions can lead to the degradation of the UV filters and, as a consequence, they can lose their ability to protect against UVB–UVA, considerably decreasing the effectiveness of the sunscreen. In addition, these undesirable photoproducts can cause adverse effects, such as allergy and phototoxicity (Scarpin et al. 2021; Nash and Tanner. 2014). Avobenzone, as example, is known to be photo-unstable, due to the keto-enol tautomerization. The enolic form absorbs in the UVA range, and the diketo form absorbs in the UVC range (Pinto da Silva et al. 2014). Some photoallergic reactions of avobenzone have been studied and correlated with its photodegradation products arylglyoxals and benzyls (Scarpin et al. 2021; Afonso et al. 2014; Karlsson et al. 2009).

With that in mind, it is evident the importance of research for new more photostable UV filters not only to ensure sunscreen effectiveness against the harmful effects of UV radiation, but also minimize the risk of skin reactions, making sun protection safer and more reliable.

### Toxicity assessment

#### Phototoxicity assay (3T3 NRU-PT)

This assay is based on a comparison of the cytotoxicity of a chemical when tested in the presence and in the absence

of exposure to a non-cytotoxic dose of simulated solar light (OECD, 2019). The results obtained in this assay are presented in Table 5 and indicate that the control norfloxacin was classified as phototoxic, according to the OECD TG 432, showing an MPE > 0.15, and non-cytotoxic due to IC<sub>50</sub> (-UV) not detected. Agonodepside B (6) and its Fraction F were evaluated at a maximum concentration of 100 µg/mL and were considered non-phototoxic (MPE < 0.10). A negative 3T3 NRU-PT result at sufficiently high concentrations is therefore regarded a sufficient stand-alone indicator for acute photosafety, while a positive result in the 3T3 NRU-PT is always a call for further considerations and probably further testing (Liesch et al. 2005; Ceridono et al. 2012). However, agonodepside B (6) showed values of IC<sub>50</sub> (-UV) of 17.8 and 12.8 µg/mL and its Fraction F showed values of IC<sub>50</sub> (-UV) of 7.1 and 6.2 µg/mL, both considered to be cytotoxic in 3T3 NRU-PT assay (Fig. 5, Table 5), which may be due to the presence of xanthenes, that are known for its cytotoxicity (El-Seedi et al. 2010; Le Pogam and Boustie 2016; Bedi et al., 2021). 3T3 fibroblast cells present higher sensitivity than keratinocytes and low IC<sub>50</sub> values do not correlate to irritant potential and thus compounds were submitted to HET-CAM assay to predict irritant potential.

#### Ocular irritation potential (HET-CAM assay)

The HET-CAM assay is a useful test for the screening of eye irritation potential of natural compounds, complementing the in vitro tests for toxicity (Thiesen et al. 2017; a, b; Maia Campos et al. 2019; Rangel et al. 2020). As expected, 0.9% NaCl (negative control) did not cause any irritation event, and 1% SDS solution (positive control) caused hemorrhage on the CAM, with an IS of 12 ± 0 and was classified as a severe irritant. The 0.01% Fraction F solution did not induce any irritant events in CAM during the period of observation, and presented a IS of 0 ± 0, being classified as non-irritant. However, 0.01% Compound 6 was classified as a slight irritant due to hyperemia observed in CAM after application, presenting a IS of 1.5 ± 1.7. The results are shown in Fig. 6 and Table 6.

**Table 5** Results of the phototoxicity assay on 3T3 NRU. IC<sub>50</sub> half maximal effective concentration, (-UV) non-irradiated, ND values not determined

Sample	Run	MPE	IC <sub>50</sub> (-UV) µg mL <sup>-1</sup>	Result
Agonodepside B (6)	1	0.056	17.79	Non-phototoxic/ Cytotoxic
	2	0.081	12.84	
Fraction F	1	0.014	7.1	Non-phototoxic/ Cytotoxic
	2	0.027	6.2	
Norfloxacin	1	0.526	ND	Phototoxic/Non- cytotoxic
	2	0.511	ND	

**Table 6** IS and classification of the effects of the 0.01% Fraction F and 0.01% Compound 6 from *Arthrinium* sp. in the HET-CAM assay. The 1% SDS and 0.9% NaCl solutions were used as positive and negative controls, respectively

Sample	Irritation Score	Classification
1% SDS	12 ± 0	Severe Irritant
0.9% NaCl	0 ± 0	Non-irritant
0.01% Fraction F	0 ± 0	Non-irritant
0.01% Compound 6	1.5 ± 1.7	Slight Irritant

## Photoprotection against UVA-induced ROS production

### HaCaT antioxidant activity

Although being considered cytotoxic in 3T3 NRU-PT assay, probably due to the higher sensibility of the monolayer model of fibroblast cells Tavares et al. (2020a, b), Fraction F maintained the cells viability around 100.03% ± 7.8 in the concentration of 10.0 µg/mL, and its isolated compound, agonodepside B (6), proved to be non-cytotoxic for HaCaT cells, with a viability around 97.2% ± 4.7 at the concentration of 10.0 µg/mL. The graph showing the results of the viability test and comparison with untreated cells and cytotoxic control are shown in Fig. 7. SDS cytotoxic control presented a cell viability of 6%

After establishing the safe concentrations to use, the antioxidant potential of Fraction F and agonodepside B (6) in HaCaT keratinocytes was assessed by detecting UVA-induced intracellular ROS using DCFH<sub>2</sub>-DA probe. Quercetin was used as an antioxidant control, resulting in a 71% ± 7.8 decrease in ROS generation, and norfloxacin as a

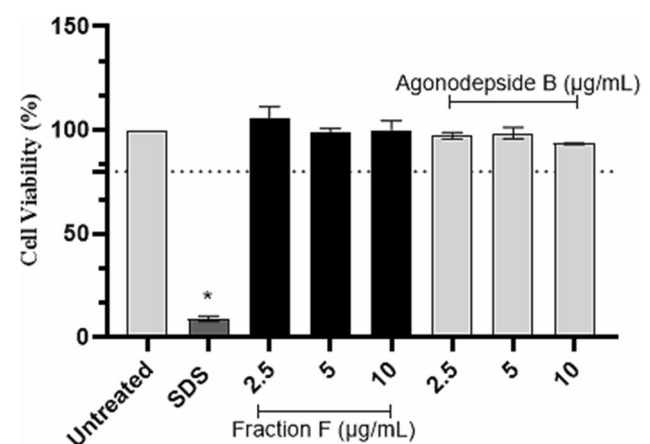


**Fig. 7** Cell viability (%) of Fraction F and agonodepside B (6) at different concentrations. The results are expressed as mean ± standard errors of the mean of three independent experiments (n = 3). Where “\*” means statistically different from untreated control (p < 0.05)

pro-oxidant control, resulting in a  $39.5\% \pm 24.5$  increase in ROS production.

According to Fig. 8, Fraction F presented an antioxidant activity statistically equal to quercetin ( $p > 0.05$ ) when tested at  $10.0 \mu\text{g/mL}$ , with a reduction around  $66.7\% \pm 14$  in UVA-induced ROS production. On the other hand, lower concentrations of Fraction F, 2.5 and  $5.0 \mu\text{g/mL}$ , did not protect against UVA-induced ROS production ( $p > 0.05$ ) ( $3.22\% \pm 3.6$  and  $10.9\% \pm 20.9$  fluorescence reduction, respectively). The isolated substance agonodepside B (**6**) did not present antioxidant activity in the lowest concentrations, 2.5 and  $5.0 \mu\text{g/mL}$ , resulting in an increase of  $6.6\% \pm 4.5$  and  $10\% \pm 2.9$  in ROS generation, respectively. However, in a similar manner as Fraction F, at the highest concentration tested ( $10.0 \mu\text{g/mL}$ ), it was able to protect from intracellular UVA-induced ROS production, with a decrease in the fluorescence of  $50.4\% \pm 5.1$ , being statistically equal to the positive control quercetin ( $p > 0.05$ ) and different from the untreated control ( $p < 0.05$ ).

The antioxidant activity of the fraction F can be explained by the presence of phenols, polyphenols derivatives, such as those isolated and identified in our research (**2–6**). The isolated compound under study agonodepside B (**6**) is also a polyphenolic structure, which also justifies its antioxidant activity similar to quercetin. Phenolic compounds are capable of donating electrons or hydrogen atoms, thereby neutralizing ROS (Souza et al. 2019; Silva et al. 2022). A wide range of antioxidants from marine fungi have been reported, such as the already mentioned phenolic compounds, and also anthraquinones, xanthenes, carotenoids, indole derivatives

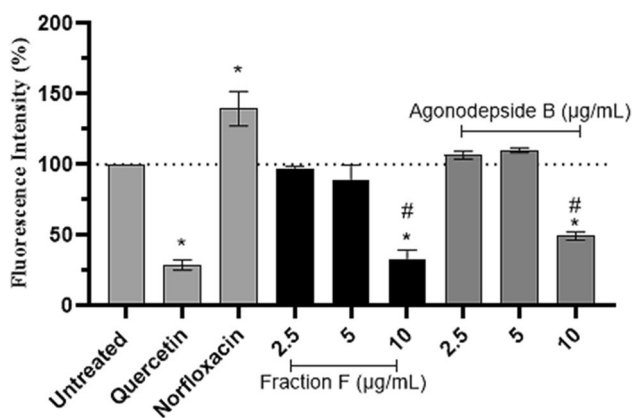


**Fig. 8** Effects of the pretreatment of HaCaT cells for a period of 24 h on ROS generation induced by UVA irradiation ( $4 \text{ J/cm}^2$ ). The results are expressed as % fluorescence. The cells were pretreated with: quercetin ( $10 \mu\text{g/mL}$ ), norfloxacin ( $100 \mu\text{g/mL}$ ); Untreated irradiated control (100% fluorescence); Fraction F (2.5, 5,  $10 \mu\text{g/mL}$ ); Agonodepside B (2.5, 5,  $10 \mu\text{g/mL}$ ). The results are expressed as mean  $\pm$  standard errors of the mean of three independent experiments ( $n=3$ ). Where “\*” means statistically different from untreated irradiated control ( $p < 0.05$ ), and “#” means statistically equal to quercetin ( $p > 0.05$ )

and alkaloids (Vitale et al. 2020). The use of natural fungal and algal products in cosmetic formulations could present advantages when compared to synthetic antioxidants, as they are derived from sustainable sources, may not harm the environment, and also be obtained from large-scale fermentation in case of the fungi growth (Vitale et al. 2020).

### Reconstructed Human Skin Model (RHS) antioxidant activity

Reconstructed human skin models are composed of a differentiated epidermis, with a corneal stratification and a living dermis. Thus, the concentrations of  $10 \mu\text{g/mL}$  of compound agonodepside B (**6**) and Fraction F were tested to evaluate the protection against UVA-induced intracellular ROS production in the reconstructed human skin model in order to mimic topical application in a physiologically relevant model that consider skin bioavailability of the tested compounds (Roguet et al. 1994; Afaq et al. 2009; Lee et al. 2017).

According to Fig. 9, the results demonstrated that UVA radiation increased ROS generation in the untreated irradiated reconstructed human skin control (NT+UV) (100%) when compared to the untreated and non-irradiated control (NT-UV), while the vehicle (PBS and ethanol 2%) was not capable of reducing ROS generation, with a fluorescence around 85.7%. The Fraction F and compound (**6**) were able to protect viable epidermis against UVA-induced ROS production, with a reduction of 34.6% and 30.2% in the fluorescence, respectively, both when tested at  $10.0 \mu\text{g/mL}$ . As mentioned, this antioxidant activity can be due to the presence of polyphenolic compounds capable of neutralizing free radicals and other ROS (Souza et al. 2019; Silva et al. 2022), which is in agreement with the protection observed in HaCaT keratinocytes.

### Conclusions

The crude extract (CE) and fraction F from the Antarctic fungus *Arthrinium* sp. showed a good absorption in both UVA I and II and UVB range (280–400 nm). From the CE, we obtained nine fractions (A–I) and focused on the study of fraction E due to its non-complex chromatogram and also sample amount. We also focused on fraction F, which showed a more complex chromatogram than E, but showed excellent UVA–UVB absorbance as well as a high UVA/UVB ratio and high “star” rating, similar to commercially available broadband UV filters. From these two fractions, six compounds were isolated and characterized, three of them not yet reported in *Arthrinium* species (**1**, **2** and **6**). These 6 compounds did not exhibit an excellent absorbance profile in the UVB–UVA range compared to the CE and Fraction

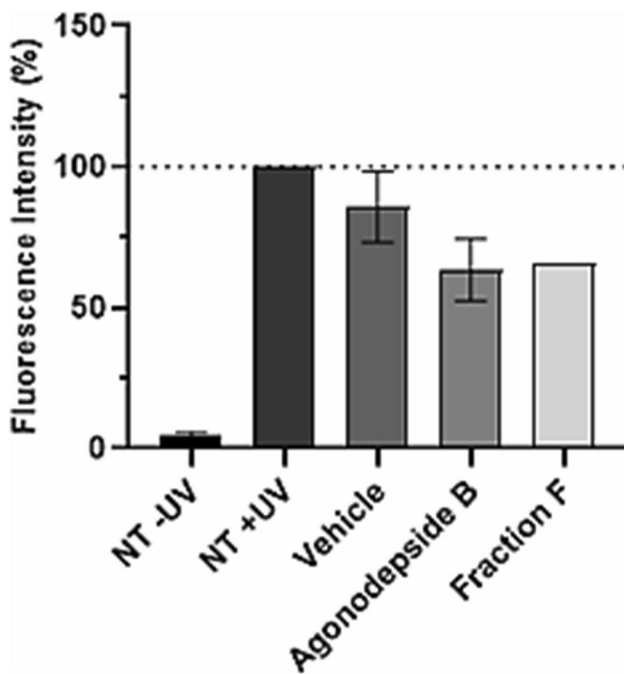


**Fig. 9** Protection against UVA-induced intracellular ROS production in reconstructed human skin models treated with agonodepside B (**6**) and Fraction F (10.0 µg/mL) and the vehicle PBS with ethanol 2%. NT +UV: irradiated non-treated control; NT -UV: non-irradiated non-treated control

F. Among them, agonodepside B (**6**) was chosen to proceed with the biological assays due to its predominance in fractions E and F, which contributed to its selection for further investigations. Agonodepside B (**6**) can also be responsible for some synergistic interaction with other compound, what gives the potential UV absorbance of fraction F. Compound **6** also demonstrated to be photostable, non-cytotoxic to HaCaT cells and was classified as a slight irritant in HET-CAM assay; it also did not present any phototoxic potential according to OECD TG 432. Besides that, it was able to protect viable epidermis against UVA-induced ROS production, both in keratinocyte monolayers and in reconstructed human skin models, with a reduction of 30.2% in the fluorescence in 3D skin models. Fraction F presented higher absorption in both UVB (280–320 nm) and UVA I and II (320–400 nm) ranges than agonodepside B (**6**), which can be due to synergism of other compounds present in the fraction. This fraction was also considered photostable, non-cytotoxic to HaCaT cells, non-irritant in HET-CAM assay and not phototoxic. Furthermore, it was also able to protect viable epidermis against UVA-induced ROS production, both in keratinocyte monolayers (effect similar to quercetin) and in reconstructed human skin models. Thus, fraction F of Antarctic fungus *Arthrimum* sp. presents the best photoprotective potential and has the advantage that it does not need further purifications to obtain the proposed safety and

efficacy. However, other clinical studies should be performed to confirm its photoprotective and antioxidant potential.

**Acknowledgements** The authors are thankful to University of São Paulo for providing access to necessary resources, the financial and fellowship support from the Brazilian research funding agencies Coordenação de Aperfeiçoamento de Pessoal de Nível Superior (CAPES) and Conselho Nacional de desenvolvimento Científico e Tecnológico (CNPq). The Department of Biomolecular Sciences and the Núcleo de Pesquisas em Produtos Naturais e Sintéticos–NPPNS are acknowledged. In the final review of the manuscript, the authors utilized an AI-powered language model known as CHAT-GPT for assistance, primarily focusing on English grammar, vocabulary, and minor content review.

**Author contributions** ACJ: Conceptualization, Methodology, Formal analysis, Investigation, Data Curation, Writing—Original Draft, Review and Editing, Visualization GSS, TRT, AJPG, CBSA, LT and KCP: Methodology, Formal analysis, Data Curation, Review and Editing MRZK: Conceptualization, Resources, Supervision LRG: Conceptualization, Resources, Supervision, Review and Editing, Project Administration PC: Resources, Project administration, Funding Acquisition HMD: Conceptualization, Resources, Review and Editing, Supervision, Project administration, Funding acquisition.

**Funding** This study had financial and logistic support from the Brazilian Antarctic Program PROANTAR/MCTI/CNPq N°64/2013), Brazilian Marine Force, National Institute of Science and Technology (INCT:BioNat), Grant #465637/2014-0, and the State of São Paulo Research Foundation (FAPESP), Grant #2014/50926-0 and 2017/03552-5.

**Availability of data and material** The raw data supporting the information of this article will be made available by the authors upon request.

## Declarations

**Conflict of interest** The authors declare no conflict of interest.

**Ethics approval** All experimental procedures involving humans were performed in accordance with the principles of the Declaration of Helsinki and were approved by the Human Research Ethics Committee of School of Pharmaceutical Sciences of Ribeirão Preto, São Paulo, Brazil (CAAE number 31758619.5.0000.5403). The written informed consent was signed by all the donors or their parents or legal guardian.

## References

- Abdel-Lateff A, Klemke C, König GM, Wright AD (2003) Two new xanthone derivatives from the algicolous marine fungus *Wardomyces anomalus*. *J Nat Prod* 66:706–708. <https://doi.org/10.1021/np020518b>
- Afaq F, Zaid MA, Khan N, Dreher M, Mukhtar H (2009) Protective effect of pomegranate-derived products on UVB-mediated damage in human reconstituted skin. *Exp Dermatol* 18:553–561. <https://doi.org/10.1111/j.1600-0625.2008.00829.x>
- Afonso S, Horita K, Sousa e Silva JP, Almeida IF, Amaral MH, Lobão PA, Costa PC, Miranda MS, Esteves da Silva JC, Sousa Lobo JM (2014) Photodegradation of avobenzone: stabilization effect of antioxidants. *J Photochem Photobiol B* 140:36–40. <https://doi.org/10.1016/j.jphotobiol.2014.07.004>
- Alfaro C, Urios A, González MC, Moya P, Blanco M (2003) Screening for metabolites from *Penicillium novae-zeelandiae* displaying

- radical-scavenging activity and oxidative mutagenicity: isolation of gentisyl alcohol. *Mutat Res* 539:187–194. [https://doi.org/10.1016/s1383-5718\(03\)00166-9](https://doi.org/10.1016/s1383-5718(03)00166-9)
- Badiali C, Petrucci V, Brasili E, Pasqua G (2023) Xanthenes: biosynthesis and trafficking in plants. *Fungi Lichens Plants* 12(4):694. <https://doi.org/10.3390/plants12040694>
- Bedi A, Gupta MK, Conlan XA, Cahill DM, Deshmukh SK (2021) Chapter 2 - Endophytic and marine fungi are potential sources of antioxidants. In: Sharma VK, Shah MP, Parmar S, Kumar A (eds) *Fungi Bio-Prospects in Sustainable Agriculture, Environment and Nano-technology*. Academic Press, Cambridge
- Bedoux G, Hardouin K, Burlot AS, Bourgougnon N (2014) Bioactive components from seaweeds: cosmetic applications and future development. *Adv Bot Res* 71:345–378. <https://doi.org/10.1016/B978-0-12-408062-1.00012-3>
- Benson DA, Cavanaugh M, Clark K, Karsch-Mizrachi I, Lipman DJ, Ostell J, Sayers EW (2013) GenBank. *Nucleic Acids Res* 41:D36–424. <https://doi.org/10.1093/nar/gks1195>
- Birch AJ, Donovan FW (1953) Studies in relation to biosynthesis. I. Some possible routes to derivatives of orcinol and phloroglucinol. *Aust J Chem* 6:360–368. <https://doi.org/10.1071/CH9530360>
- Cao S, Lee AS, Huang Y, Flotow H, Ng S, Butler MS, Buss AD (2002) Agonodepsides A and B: two new depsides from a filamentous fungus F7524. *J Nat Prod* 65:1037–1038. <https://doi.org/10.1021/np010626i>
- Castenholz RW (1988) [3] Culturing methods for cyanobacteria. *Methods Enzymol* 167:68. [https://doi.org/10.1016/0076-6879\(88\)67004-2](https://doi.org/10.1016/0076-6879(88)67004-2)
- Ceridono M, Tellner P, Bauer D, Barroso J, Alépée N, Corvi R, De Smedt A, Fellows MD, Gibbs NK, Heisler E, Jacobs A, Jirova D, Jones D, Kandárová H, Kasper P, Akunda JK, Krul C, Learn D, Wilcox P (2012) The 3T3 neutral red uptake phototoxicity test: practical experience and implications for phototoxicity testing—the report of an ECVAM-EFPIA workshop. *Regul Toxicol Pharmacol* 63:480–488. <https://doi.org/10.1016/j.yrtph.2012.06.001>
- Cordero RR, Feron S, Damiani A, Redondas A, Carrasco J, Sepúlveda E, Jorquera J, Fernandez F, Llanillo P, Rowe PM, Seckmeyer G (2022) Persistent extreme ultraviolet irradiance in Antarctica despite the ozone recovery onset. *Sci Rep* 12:1266. <https://doi.org/10.1038/s41598-022-05449-8>
- DiNardo JC, Downs CA (2018) Dermatological and environmental toxicological impact of the sunscreen ingredient oxybenzone/benzophenone-3. *J Cosmet Dermatol* 17:15–19. <https://doi.org/10.1111/jocd.12449>
- Ding J, Wu B, Chen L (2022) Application of marine microbial natural products in cosmetics. *Front Microbiol* 13:892505. <https://doi.org/10.3389/fmicb.2022.892505>
- dos Santos GS, Teixeira TR, Colepicolo P, Debonsi HM (2021) Natural products from the poles: structural diversity and biological activities. *Rev Bras Farmacog* 31(5):531–560. <https://doi.org/10.1007/s43450-021-00203-z>
- El-Seedi HR, El-Barbary MA, El-Ghorab DM, Bohlin L, Borg-Karlson AK, Göransson U, Verpoorte R (2010) Recent insights into the biosynthesis and biological activities of natural xanthenes. *Curr Med Chem* 17:854–901. <https://doi.org/10.2174/092986710790712147>
- Fernandes A, Da S, Alencar AS, Evangelista H, Mazzei JL, Felzenszwalb I (2015) Photoprotective and toxicological activities of extracts from the Antarctic moss *Sanionia uncinata*. *Pharmacogn Mag* 11(41):38–43. <https://doi.org/10.4103/0973-1296.149701>
- Fivenson D, Sabzevari N, Qiblawi S, Blitz J, Norton BB, Norton SA (2020) Sunscreens: UV filters to protect us: Part 2-Increasing awareness of UV filters and their potential toxicities to us and our environment. *Int J Womens Dermatol* 7:45–69. <https://doi.org/10.1016/j.ijwd.2020.08.008>
- Gaspar LR, Maia Campos PMBG (2006) Evaluation of the photostability of different UV filter combinations in a sunscreen. *Int J Pharm* 307:123–128. <https://doi.org/10.1016/j.ijpharm.2005.08.029>
- Gaspar LR, Tharmann J, Maia Campos PMBG, Liebsch M (2013) Skin phototoxicity of cosmetic formulations containing photounstable and photostable UV-filters and vitamin a palmitate. *Toxicol in Vitro* 27:418–425. <https://doi.org/10.1016/j.tiv.2012.08.006>
- Gremaud G, Tabacchi R (1994) Isocoumarins of the Fungus *Ceratomyces Fimbriata coffea*. *Nat Prod Let* 5(2):95–103. <https://doi.org/10.1080/10575639408044041>
- He H, Li A, Li S, Tang J, Li L, Xiong L (2021) Natural components in sunscreens: Topical formulations with sun protection factor (SPF). *Biomed Pharmacother* 134:111161. <https://doi.org/10.1016/j.biopha.2020.111161>
- Heo YM, Kim K, Ryu SM, Kwon SL, Park MY, Kang JE, Kim J-J (2018) Diversity and ecology of marine algal arthrinium species as a source of bioactive natural products. *Mar Drugs* 16(12):508. <https://doi.org/10.3390/md16120508>
- Kalyanaraman B, Darley-Usmar V, Davies KJ, Dennery PA, Forman HJ, Grisham MB, Mann GE, Moore K, Roberts LJ 2nd, Ischiropoulos H (2012) Measuring reactive oxygen and nitrogen species with fluorescent probes: challenges and limitations. *Free Radic Biol Med* 52:1–6. <https://doi.org/10.1016/j.freeradbiomed.2011.09.030>
- Karlsson I, Hillerström L, Stenfeldt AL, Mårtensson J, Börje A (2009) Photodegradation of dibenzoylmethanes: potential cause of photocontact allergy to sunscreens. *Chem Res Toxicol* 22(11):1881–1892. <https://doi.org/10.1021/tx900284e>
- Kealey JT, Craig JP, Barr PJ (2021) Identification of a lichen depside polyketide synthase gene by heterologous expression in *Saccharomyces cerevisiae*. *Metab Eng Commun* 13:e00172. <https://doi.org/10.1016/j.mec.2021.e00172>
- Le Pogam P, Boustie J (2016) Xanthenes of lichen source: a 2016 update. *Molecules* 21:294. <https://doi.org/10.3390/molecules21030294>
- Lee M, Hwang JH, Lim KM (2017) Alternatives to *In Vivo* Draize rabbit eye and skin irritation tests with a focus on 3D reconstructed human cornea-like epithelium and epidermis models. *Toxicol Res* 33:191–203. <https://doi.org/10.5487/TR.2017.33.3.191>
- Legaz EM, de Armas R, Vicente C (2011) Bioproduction of depsidones for pharmaceutical purposes. In: Rundfeldt C (ed) *Drug development – a case study based insight into modern strategies*. Rijeka, In Tech
- Li G, Dickschat JS, Guo YW (2020) Diving into the world of marine 2,11-cyclized cembranoids: a summary of new compounds and their biological activities. *Nat Prod Rep* 37:1367–1383. <https://doi.org/10.1039/D0NP00016G>
- Liebsch M, Spielmann H, Pape W, Krul C, Deguercy A, Eskes C (2005) UV-induced effects. *Altern Lab Anim* 33:131–146. <https://doi.org/10.1177/026119290503301s14>
- Maia Campos PMBG, Benevenuto CG, Calixto LS, Melo MO, Pereira KC, Gaspar LR (2019) *Spirulina, Palmaria Palmata, Cichorium Intybus*, and *Medicago Sativa* extracts in cosmetic formulations: an integrated approach of in vitro toxicity and in vivo acceptability studies. *Cutan Ocul Toxicol* 38:1–25. <https://doi.org/10.1080/15569527.2019.1579224>
- Marionnet C, Pierrard C, Golebiewski C, Bernerd F (2014) Diversity of biological effects induced by longwave UVA rays (UVA1) in reconstructed skin. *PLoS ONE* 9:e105263. <https://doi.org/10.1371/journal.pone.0105263>
- Mitchelmore CL, Burns EE, Conway A, Heyes A, Davies IA (2021) A critical review of organic ultraviolet filter exposure, hazard, and risk to corals. *Environ Toxicol Chem* 40:967–988. <https://doi.org/10.1002/etc.4948>






- Nash JF (2014) Tanner PR Relevance of UV filter/sunscreen product photostability to human safety. *Photodermatol Photoimmunol Photomed* 30:88–95. <https://doi.org/10.1111/phpp.12113>
- Noor AO, Almasri DM, Bagalagel AA, Abdallah HM, Mohamed SGA, Mohamed GA, Ibrahim SRM (2020) Naturally occurring isocoumarins derivatives from endophytic fungi: sources, isolation, structural characterization, biosynthesis, and biological activities. *Molecules* 25:395. <https://doi.org/10.3390/molecules25020395>
- Núñez-Pons L, Avila C, Romano G, Verde C, Giordano D (2018) UV-protective compounds in marine organisms from the Southern Ocean. *Mar Drugs* 16(9):336. <https://doi.org/10.3390/md16090336>
- Ogaki MB, de Paula MT, Ruas D, Pellizzari FM, García-Laviña CX, Rosa LH (2019) Marine fungi associated with Antarctic Macroalgae. In: Castro-Sowinski S (ed) *The ecological role of microorganisms in the Antarctic environment*. Springer, Cham
- OECD- Organization for Economic Co-operation and Development, OECD guidelines for testing of chemicals test n°. 432: In vitro 3T3 NRU Phototoxicity Test (2019b) Available at: <https://doi.org/10.1787/9789264071162-en> Accessed: 22 Jun 22
- Overgaard ML, Aalborg T, Zeuner EJ, Westphal KR, Lau F, Nielsen VS, Carstensen KB, Hundebøll EA, Westermann TA, Rathsach GG, Sørensen JL, Frisvad JC, Wimmer R, Sondergaard TE (2023) Quick guide to secondary metabolites from *Apiospora* and *Arthrinium*. *Fungal Biol Rev* 43:100288. <https://doi.org/10.1016/j.fbr.2022.10.001>
- Pal S, Chatare V, Pal M (2011) Isocoumarin and its derivatives: an overview on their synthesis and applications. *Curr Org Chem* 15:782. <https://doi.org/10.2174/138527211794518970>
- Pennacchi PC, de Almeida ME, Gomes OL, Faião-Flores F, de Araújo Crepaldi MC, Dos Santos MF, de Moraes Barros SB, Maria-Engler SS (2015) Glycated reconstructed human skin as a platform to study the pathogenesis of skin aging. *Tissue Eng Part A* 21:2417–2425. <https://doi.org/10.1089/ten.tea.2015.0009>
- Pinto da Silva L, Ferreira PJ, Duarte DJ, Miranda MS, Esteves da Silva JC (2014) Structural, energetic, and UV-Vis spectral analysis of UVA filter 4-tert-butyl-4'-methoxydibenzoylmethane. *J Phys Chem A* 118:1511–1518. <https://doi.org/10.1021/jp4123375>
- Pintos Á, Alvarado P (2021) Phylogenetic delimitation of *Apiospora* and *Arthrinium*. *Fungal Sys and Evolution* 7(1):197–221. <https://doi.org/10.3114/fuse.2021.07.10>
- Pivetta TP, Silva LBD, Kawakami CM, Araújo MM, Del Lama MPF, de M, Naal RMZG, Maria-Engler SS, Gaspar LR, Marcato PD, (2019) Topical formulation of quercetin encapsulated in natural lipid nanocarriers: Evaluation of biological properties and phototoxic effect. *J Drug Deliv Sci Technol* 53:1–11. <https://doi.org/10.1016/j.jddst.2019.101148>
- Rangel KC, Villela LZ, de Pereira K, C, Colepicolo P, Debonsi HM, Gaspar LR, (2020) Assessment of the photoprotective potential and toxicity of Antarctic red macroalgae extracts from *Curdiea racovitzae* and *Iridaea cordata* for cosmetic use. *Algal Res* 50:1–13. <https://doi.org/10.1016/j.algal.2020.101984>
- Rasmussen C, Gratz K, Liebel F, Southall M, Garay M, Bhattacharyya S, Simon N, Vander Zanden M, Van Winkle K, Pirnstill J, Pirnstill S, Comer A, Allen-Hoffmann BL (2010) The StrataTest® human skin model, a consistent in vitro alternative for toxicological testing. *Toxicol in Vitro* 24:2021–2029. <https://doi.org/10.1016/j.tiv.2010.07.027>
- Roberts JC (1961) Naturally occurring xanthenes. *Chem Rev* 61:591–605. <https://doi.org/10.1021/cr60214a003>
- Roguet R, Régnier M, Cohen C, Dossou KG, Rougier A (1994) The use of in vitro reconstituted human skin in dermatotoxicity testing. *Toxicol in Vitro* 8:635–639. [https://doi.org/10.1016/0887-2333\(94\)90033-7](https://doi.org/10.1016/0887-2333(94)90033-7)
- Rosic NN (2021) Recent advances in the discovery of novel marine natural products and mycosporine-like amino acid UV-absorbing compounds. *Appl Microbiol Biotechnol* 105(19):7053–7067. <https://doi.org/10.1007/s00253-021-11467-9>
- Saeed A (2016) Isocoumarins, miraculous natural products blessed with diverse pharmacological activities. *Eur J Med Chem* 116:290–317. <https://doi.org/10.1016/j.ejmech.2016.03.025>
- Saewan N, Jimtaisong A (2015) Natural products as photoprotection. *J Cosmet Dermatol* 14:47–63. <https://doi.org/10.1111/jocd.12123>
- Sarasan M, Puthumana J, Job N, Han J, Lee JS, Philip R (2017) Marine algicolous endophytic fungi—a promising drug resource of the era. *J Microbiol Biotechnol* 27:1039–1052. <https://doi.org/10.4014/jmb.1701.01036>
- Scarpin MS, Kawakami CM, Rangel KC, Pereira KC, Benevenuto CG, Gaspar LR (2021) Effects of UV-filter photostabilizers in the photostability and phototoxicity of vitamin A palmitate combined with avobenzone and octyl methoxycinnamate. *Photochem Photobiol* 97:700–709. <https://doi.org/10.1111/php.13407>
- SCCS - Scientific Committee on Consumer Safety, The SCCS notes of guidance for the testing of cosmetic ingredients and their safety evaluation (2018). [https://ec.europa.eu/health/sites/health/files/scientific\\_committees/consumer\\_safety/docs/sccs\\_o\\_224.pdf](https://ec.europa.eu/health/sites/health/files/scientific_committees/consumer_safety/docs/sccs_o_224.pdf) Accessed: 22 Jun 22
- Silva EP, Herminio VLdQ, Motta DN, Soares MBP, Rodrigues LdAP, Viana JD, Freitas FA, Silva APG, Souza FDCdA, Vilas Boas EVdB (2022) The role of phenolic compounds in metabolism and their antioxidant potential. *Res Soc Dev* 11(10):297111031750. <https://doi.org/10.33448/rsd-v11i10.31750>
- Souza EL, Albuquerque TMR, Santos AS, Massa NML, De Alves JLB (2019) Potential interactions among phenolic compounds and probiotics for mutual boosting of their health-promoting properties and food functionalities—a review. *Crit Rev Food Sci Nutr* 59(10):1–15. <https://doi.org/10.1080/10408398.2018.1425285>
- Tavares RSN, Kawakami CM, Pereira KC, Amaral do GT, Benevenuto CG, Maria-Engler SS, Colepicolo P, Debonsi HM, Gaspar LR (2020a) Fucoxanthin for topical administration, a phototoxic vs photoprotective potential in a tiered strategy assessed by in vitro methods. *Antioxidants* 9:328. <https://doi.org/10.3390/antiox9040328>
- Tavares RSN, Maria-Engler SS, Colepicolo P, Debonsi HM, Schäfer-Korting M, Marx U, Gaspar LR, Zoschke C (2020b) Skin irritation testing beyond tissue viability: fucoxanthin effects on inflammation, homeostasis, and metabolism. *Pharmaceutics* 12:136. <https://doi.org/10.3390/pharmaceutics12020136>
- Teixeira TR, dos Santos GS, Turatti ICC, Piazini MH, von Kress MR, Z, Colepicolo P, Debonsi HM, (2019) Characterization of the lipid profile of Antarctic brown seaweeds and their endophytic fungi by gas chromatography–mass spectrometry (GC–MS). *Polar Biol* 42:1431–1444. <https://doi.org/10.1007/s00300-019-02529-w>
- Thiesen LC, Baccarin T, Fischer-Muller AF, Meyre-Silva C, Couto AG, Bresolin TM, Santin JR (2017a) Photochemoprotective effects against UVA and UVB irradiation and photosafety assessment of *Litchi chinensis* leaves extract. *J Photochem Photobiol B* 167:200–207. <https://doi.org/10.1016/j.jphotobiol.2016.12.033>
- Vega J, Schneider G, Moreira BR, Herrera C, Bonomi-Barufi J, Figueroa FL (2021) Mycosporine-like amino acids from red macroalgae: UV-photoprotectors with potential cosmeceutical applications. *App Sci* 11(11):5112. <https://doi.org/10.3390/app11115112>
- Vitale GA, Coppola D, Palma Esposito F, Buonocore C, Ausuri J, Tortorella E, de Pascale D (2020) Antioxidant molecules from marine fungi: methodologies and perspectives. *Antioxidants* 9(12):1183. <https://doi.org/10.3390/antiox9121183>
- Wang SQ, Stanfield JW, Osterwalder U (2008) In vitro assessments of UVA protection by popular sunscreens available in the United States. *J Am Acad Dermatol* 59(6):934–942. <https://doi.org/10.1016/j.jaad.2008.07.043>

- Watkins YSD, Sallach JB (2021) Investigating the exposure and impact of chemical UV filters on coral reef ecosystems: review and research gap prioritization. *Integr Environ Assess Manag* 17:967–981. <https://doi.org/10.1002/ieam.4411>
- White TJ, Bruns TD, Lee SB, Taylor JW (1990) Amplification and direct sequencing of fungal ribosomal RNA genes for phylogenetics. In: Innis MA, Gelfand DH, Sninsky JJ, White TJ (eds) *PCR Protocols: a guide to methods and applications*. Academic Press, Cambridge, pp 315–322
- Zhang Y, Shah P, Wu F, Liu P, You J, Goss G (2021) Potentiation of lethal and sub-lethal effects of benzophenone and oxybenzone by UV light in zebrafish embryos. *Aquat Toxicol* 235:105835. <https://doi.org/10.1016/j.aquatox.2021.105835>

**Publisher's Note** Springer Nature remains neutral with regard to jurisdictional claims in published maps and institutional affiliations.

Springer Nature or its licensor (e.g. a society or other partner) holds exclusive rights to this article under a publishing agreement with the author(s) or other rightsholder(s); author self-archiving of the accepted manuscript version of this article is solely governed by the terms of such publishing agreement and applicable law.

## Authors and Affiliations

Ana Carolina Jordão<sup>1</sup>  · Gustavo Souza dos Santos<sup>1,5</sup>  · Thaiz Rodrigues Teixeira<sup>1,6</sup>  · Ana Júlia Pasuch Gluzek<sup>2</sup>  · Clarissa Bechuate de Souza Azevedo<sup>2</sup>  · Karina de Castro Pereira<sup>2</sup> · Ludmilla Tonani<sup>3</sup>  · Lorena Rigo Gaspar<sup>2</sup>  · Márcia Regina von Zeska Kress<sup>3</sup>  · Pio Colepicolo<sup>4</sup>  · Hosana Maria Debonsi<sup>1</sup> 

✉ Hosana Maria Debonsi  
hosana@fcfrp.usp.br

- <sup>1</sup> Department of Biomolecular Sciences, School of Pharmaceutical Sciences of Ribeirão Preto, University of São Paulo, Ribeirão Preto, SP, Brazil
- <sup>2</sup> Department of Pharmaceutical Sciences, School of Pharmaceutical Sciences of Ribeirão Preto, University of São Paulo, Ribeirão Preto, SP, Brazil
- <sup>3</sup> Department of Clinical, Toxicological and Bromatological Analysis, School of Pharmaceutical Sciences, University of São Paulo, Ribeirão Preto, SP, Brazil

<sup>4</sup> Department of Biochemistry, Chemistry Institute, University of São Paulo, São Paulo, SP, Brazil

<sup>5</sup> Department of Life Sciences, State University of Bahia, Salvador, BA, Brazil

<sup>6</sup> Center for Discovery and Innovation in Parasitic Disease, Skaggs School of Pharmacy and Pharmaceutical Sciences, University California San Diego, California, CA, USA